# A MULTIOBJECTIVE OPTIMIZATION APPROACH TO DK-ITERATION

**I. A. Griffin** [*] **P. J. Fleming** [*]

[*] *Dept. Automatic Control and Systems Engineering, The University of Sheffield, Mappin Street, Sheffield, S1 3JD, UK. Tel: +44 114 222 5250, Fax: +44 114 273 1729, E-mail: i.griffin@sheffield.ac.uk*

Abstract: The structured singular value, $\mu$, can be used to analyse the robust performance characteristics of control systems with respect to the potential perturbations in plant dynamics. $\mu$ can also be used in control system design. Whilst it is not currently possible to synthesise a truly $\mu$-optimal controller, a process known as DK-iteration is available employing $H_\infty$ design techniques. A preliminary study is described that uses a multiobjective genetic algorithm to tune the weighting functions of a controller derived using DK-iteration.

Keywords: Robust Control, Optimization, structured singular value, DK-iteration.

## 1. INTRODUCTION

The problem of ensuring that a linear controller exhibits appropriate characteristcs across the operating range of a non-linear plant is a well-studied problem within the field of Control Engineering. Standard approaches to the problem include gain-scheduling of linear control algorithm parameters and the use of non-linear control algorithms. Whilst these two approaches have been successfully applied in a wide range of application areas, they are not without difficulties. Non-linear control approaches are often the subject of low levels of confidence within certain industries. Gain-scheduling is a widely-accepted technique but does require a suitable, measurable parameter against which the controller gains can be scheduled, which may not be available.

The feasibility of designing a single, linear control algorithm for a non-linear system can be found in the literature. Previous work by the authors has involved the design of $H\infty$ Loop Shaping Design Procedure (LSDP) control algorithms to address the control requirements of a non-linear system represented by multiple, linear models. The weighting functions for the $H\infty$ LDSP controller were tuned using a genetic optimiser in order to meet the performance requirements.

This paper describes a preliminary investigation into the potential for extending this design approach by using a multiobjective genetic algorithm (MOGA) to tune the weighting functions for a $\mu$-based controller via DK-iteration. A basic introduction to both $\mu$-synthesis and MOGA are provided before two case studies are described.

## 2. ROBUSTNESS ANALYSIS

The *raison d'être* for $\mu$-design is to provide a technique for analysing and achieving robustness for controlled systems. In order to cater for the differences between a real-world plant and its model, or the differences in model parameters that may occur across a non-linear operating envelope, a method for representing and quantifying the potential parametric discrepancies is required. This involves defining a region of uncertainty within which all possible plant descriptions or parameter values are known to lie. This can be done using norm-bounded, frequency dependent transfer functions as shown in equation (1). This results in a continuous set of possible system representations containing an infinite number of transfer functions that may represent the actual system. This is a suitable format for representing lumped uncertainty (a combination of parametric and unmodelled/neglected dynamics uncertainty) as shown in equation 1.

$$G_p(s) = G(s)(1+\omega_I\Delta_I) \qquad |\Delta_I(j\omega)| \leq 1 \forall\omega (1)$$

Given this representation of uncertainty the requirements for achieving robustness can now be defined. The loop transfer function of the system, $L_p$, containing this perturbed plant is as shown in equation (2),

$$L_p = G_pK = GK(1+\omega_I\Delta_I) = L + \omega_I L\Delta_I, (2)$$
$$|\Delta_I(j\omega)| \leq 1 \qquad \forall\omega$$

where L is the nominal loop transfer function.

Based on the Nyquist stability criterion the condition for robust stability can then be defined as in equations (3), (4),

$$|\omega_I L| \leq |1+L|, \qquad \forall\omega \qquad (3)$$

which simplifies to

$$\left|\frac{\omega_I L}{1+L}\right| \leq 1, \forall\omega \quad \Leftrightarrow \quad |\omega_I T| \leq 1, \forall\omega \qquad (4)$$
$$\Leftrightarrow \quad \| \omega_I T \|_\infty \leq 1$$

Performance for both SISO and MIMO plant is often defined for the closed-loop system in terms of the sensitivity function. The sensitivity function is defined as being the closed-loop transfer function from a disturbance input to the controlled output of a system. Here we consider disturbances at the output of the plant The sensitivity function is defined in equation (5). Note that 1 is replaced by the identity matrix, I, for MIMO systems.

$$S = (1+L)^{-1} \qquad (5)$$

Given the sensitivity function's influence over disturbance signal transmission to the controlled outputs, it is desirable that it be kept small at frequency ranges over which disturbances are likely to be experienced. Performance can therefore be defined using an upper bound on the sensitivity function over the frequency range. This upper bound is the reciprocal of a weighting function, $\omega_P$, chosen by the designer as shown in equation (6) and can be manipulated as shown in equation (7)

$$|S(j\omega)| \leq \frac{1}{|\omega_P(j\omega)|}, \forall\omega \qquad (6)$$

$$|\omega_P S| \leq 1, \forall\omega \qquad \| \omega_P S \|_\infty \leq 1 \qquad (7)$$

Note: subscript P stands for performance

From equation (5) it can be seen that the sensitivity function is the reciprocal of the distance from the open-loop locus to the critical point in the Nyquist plane for any given frequency. Equation (7) can therefore be manipulated as shown in equation (8)

$$|\omega_P S| \leq 1, \forall\omega \qquad \Leftrightarrow \qquad |\omega_P| \leq |1+L|, \forall\omega (8)$$

This infers that in order to achieve the level of performance required by the designer, the open-loop locus must lie at least a distance of $|\omega_P(j\omega)|$ from the critical point, -1.

The above condition gives nominal performance. The performance requirements specified by the designer in the form of the performance weight, $\omega_P(j\omega)$, are satisfied for the case where there is no uncertainty in the plant description. In order to extend the principle to robust performance, the conditions for robust stability and nominal performance are combined as shown in equations (9), (10) and (11):

$$|\omega_P| + |\omega_I L| \leq |1+L|, \qquad \forall\omega, \qquad (9)$$
$$|\omega_P(1+L)^{-1}| + |\omega_I L(1+L)^{-1}| \leq 1, \qquad \forall\omega, (10)$$
$$max_\omega(|\omega_P S| + |\omega_I T|) \leq 1 \qquad (11)$$

Equation (11) gives the condition for robust performance. It can therefore be stated that the structured singular value, $\mu$, for robust performance is as given in equation (12)

$$\mu(N_{RP}) = |\omega_P S| + |\omega_I T|. \qquad (12)$$

This condition defines the structured singular value for robust performance in terms of N where N can be found by applying linear fractional transformations to the block diagrma of the closed-loop system shown in Figure 1.

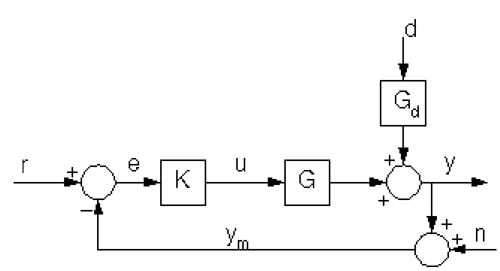


Fig. 1. One-degree-of-freedom feedback control system.

Software algorithms for the synthesis of $H_\infty$-based controllers rely on the plant being described in the general formulation given by Doyle (Doyle, 1982). This formulation is produced for the case with no plant uncertainty by defining four vectors w, z, u, and v where

$$w = \begin{bmatrix} w_1 \\ w_2 \\ w_3 \end{bmatrix} = \begin{bmatrix} d \\ r \\ n \end{bmatrix}; \qquad z = e = y - r; \quad (13)$$

$$v = r - y_m = r - y - n$$

The vectors w and u represent the inputs to the generalized plant, P, from external inputs and the controller respectively. Vectors z and v are the outputs from the generalized plant where z gives the values to be minimized and v is the output from the plant to the controller.This structure is shown in the block diagram in Figure 2

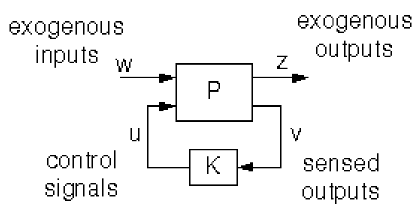


Fig. 2. Generalized control structure with no model uncertainty.

Based on the vector structures given in equation (13), the vector structures for the generalized plant, P, can now be derived for the closed-loop strucure given in Figure 1 as:-

$$z = y - r = Gu + G_d d - r \tag{14}$$

$$= G_d w_1 - I w_2 + 0 w_3 + Gu$$

$$v = r - y_m = r - Gu - G_d d - n \tag{15}$$

$$= -G_d d + I w_2 - I w_3 - Gu$$

The generalized plant, P, is therefore the transfer function matrix from $[w \quad u]^T$ to $[z \quad v]^T$ shown as:-

$$\begin{bmatrix} z \\ v \end{bmatrix} = \begin{bmatrix} G_d & -I & 0 & G \\ -G_d & I & -I & -G \end{bmatrix} \begin{bmatrix} w \\ u \end{bmatrix} \tag{16}$$

$$P = \begin{bmatrix} G_d & -I & 0 & G \\ -G_d & I & -I & -G \end{bmatrix} \tag{17}$$

The use of the generalized control structure for the synthesis problem is the process of producing a controller that minimizes a chosen norm of the plant from w to z, e.g. the $H_\infty$ norm. The structure shown in Figure 2, where P is an open-loop representation, is ideal for use in the synthesis problem. However, for analysis of the resulting closed-loop system it is preferable to form a closed-loop representation, N, that incorporates both the plant and the controller. The amalgamation process involves partitioning the generalized plant, P, into sub-matrices whose sizes are compatible with the input and output vectors and then using a lower linear fractional transformation. The partitioned plant is shown in equation (18) and the closed-loop interconnection structure is derived thus:-

$$P = \begin{bmatrix} P_{11} & P_{12} \\ P_{21} & P_{22} \end{bmatrix} \tag{18}$$

where

$$P_{11} = [\, G_d \;\; -I \;\; 0 \,], P_{12} = [G],$$

$$P_{21} = [\, -G_d \;\; I \;\; -I \,], P_{22} = [-G]$$

and

$$N = P_{11} + P_{12} K (I - P_{22} K)^{-1} P_{12} \tag{19}$$

$$= F_l(P, K)$$

Thus, the closed-loop interconnection structure, N, has been derived for the closed-loop system shown in Figure 1. Given the definitions established here, the process of DK-iteration for synthesising a $\mu$-based controller can be introduced.

## 3. DK-ITERATION

This Section addresses the design of a controller, K, for the situation shown in Figure 3. Uncertainty at the plant input and performance requirements at the system output are described by $W_I$ and $W_P$ respectively. The generalized open- and closed-loop interconnection structures for this configuration are shown and the technique known as DK-iteration for producing an $H_\infty$ controller through minimizing the $\mu$ condition is then described (Doyle, 1982).

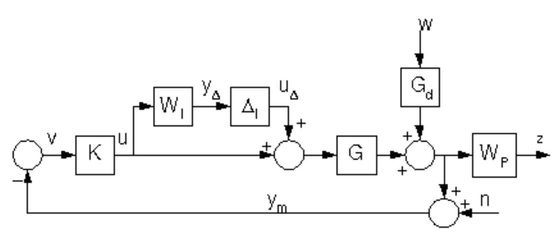


Fig. 3. Closed-loop system with uncertainty and performance weighting

For the configuration shown in Figure 3 the generalized open-loop representation can be derived using the approach shown in equations (13) to (19) and is given by equation (20):

$$\begin{bmatrix} y_\Delta \\ z \\ v \end{bmatrix} = P \begin{bmatrix} u_\Delta \\ w \\ u \end{bmatrix}$$

and

$$where \qquad P = \begin{bmatrix} 0 & 0 & W_I \\ W_P G & W_P G_d & W_P G \\ -G & -G_d & -G \end{bmatrix}, (20)$$

$$P_{11} = \begin{bmatrix} 0 & 0 \\ W_P G & W_P G_d \end{bmatrix}, \quad P_{12} = \begin{bmatrix} W_I \\ W_P G \end{bmatrix},$$

$$P_{21} = \begin{bmatrix} -G & -G_d \end{bmatrix}, \quad P_{22} = [-G]$$

Note that the input and output vectors for this configuration contain the inputs and outputs relating to the input uncertainty perturbation, $u_\Delta$ and $y_\Delta$. By applying the relationship for a lower linear fractional transformation shown in equation (19), the closed-loop interconnection structure, N, which incorporates P and K is given by equation (21).

$$N = \begin{bmatrix} -W_I K G (I+GK)^{-1} & -W_I K G_d (I+GK)^{-1} \\ W_P G (I+KG)^{-1} & W_P G_d (I+GK)^{-1} \end{bmatrix} \qquad (21)$$

In order to assess robust performance, the condition initially defined in equation (12) is evaluated. The condition for the configuration shown in Figure 3 is:-

$$\mu(N) = \mu\left(\begin{bmatrix} -W_I K G (I+GK)^{-1} & -W_I K G_d (I+GK)^{-1} \\ W_P G (I+KG)^{-1} & W_P G_d (I+GK)^{-1} \end{bmatrix}\right) \qquad (22)$$
$$= |W_I T_I| + |W_P G_d S|$$

where the disturbance model, $G_d$, is included.

DK-iteration is a controller design technique that combines $H_\infty$-synthesis with $\mu$-analysis in an effort to produce a controller that results in a minimal peak value of $\mu$ across the frequency range. An upper bound on $\mu$ is therefore defined. A scaling matrix, D, is chosen such that it commutes with $\Delta$, the plant perturbation, i.e. $D\Delta = \Delta D$. An upper bound on $\mu$ for robust performance can then be defined as:-

$$\mu(N) \leq min_{D \in D} \overline{\sigma}(DND^{-1}) \qquad (23)$$

The synthesis problem is then to find the controller, K, that minimizes this upper bound over the frequency range i.e.

$$min_K (min_{D \in D} \parallel DN(K)D^{-1} \parallel_\infty) \qquad (24)$$

This is done by minimizing the condition shown in equation 24 with respect to either K and D alternately.

DK-iteration then proceeds according to the following steps as shown in (Skogestad & Postlethwaite, 1996):

(1) K-step: Synthesize an $H_\infty$ controller for the scaled problem, $min_K \parallel DN(K)D^{-1} \parallel_\infty$ with fixed D(s).
(2) D-step: Find $D(j\omega)$ to minimize at each frequency $\overline{\sigma}(DND^{-1}(j\omega))$ with respect to N.
(3) Fit the magnitude of each element of $D(j\omega)$ to a stable and minimum phase transfer function D(s) and go to Step 1.

Designer interaction with the $\mu$-synthesis procedure involves adjusting parameters in the uncertainty and/or performance weights with the aim of achieving a peak $\mu$ value close to 1. This would imply that robust performance across the operating envelope in question had been achieved for the performance requirements specified.

## 4. MULTIOBJECTIVE OPTIMIZATION USING GENETIC ALGORITHMS

The genetic algorithm (GA) is a stochastic global search method which employs a Darwinian, 'survival of the fittest' principle. At each generation a population of potential solutions is assessed in terms of their performance in the problem domain. These individuals are then ranked according to their performance, the fittest having the highest probability of breeding. Pairs of individuals are then chosen according to these probabilities and bred together. Their offspring form the subsequent generation of potential solutions. A mutation operator is also implemented randomly in order to ensure that the probability of searching any given section of the search space is never zero. As this cycle repeats over a number of generations, the population becomes more refined as the least fit individuals are rejected and an optimal solution is approached. The steps involved in the execution of a genetic algorithm can be summarised as follows:

- The genotypic representation, often encoded in binary as for all studies carried out in this thesis, of an initial population is randomly generated.
- These genotypic representations are converted to the corresponding phenotypes or decision variables.
- The performance of each member of the population is assessed in turn using a prescribed objective function.
- Each individual is assigned a fitness value according to its objective function value.

- Individuals are selected for reproduction according to a stochastic selection procedure with probabilities derived from their fitness function values.
- Individuals genotypic representations are bred using specified mechanisms such as crossover.
- A mutation operator is then applied stochastically to the genotypic representations of the offspring in order to ensure that the probability of investigating any given area of the search space is never zero.
- The newly generated population is then assessed according to its objective function performance, the GA operations are repeated and new generations evolved until a termination criterion is satisfied.

The multiobjective genetic algorithm (MOGA) is implemented using a standard GA (Fonseca & Fleming, 1995) with extensions for multiobjective ranking, fitness sharing and mating restrictions. A multiobjective optimiser is employed for the case studies considered later in order to address the multiple, conflicting requirements of the problems in question. The salient features of MOGA are shown in Fig. 4 and described below.

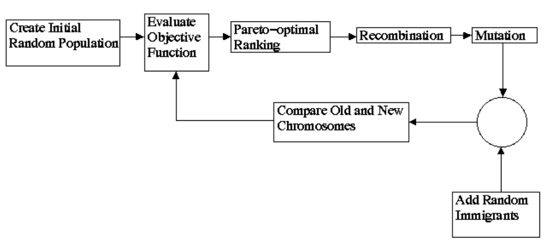


Fig. 4. The MOGA

Multiobjective ranking is based on the concept of the dominance of an individual and Paret-optimality. This system of ranking is non-unique; for example a number of individuals are ranked zero and these are said to be non-dominated. Ranking may also be combined with goal and/or priority information to discriminate between non-dominated solutions. For example, a solution in which all the goals are satisfied may be considered superior, or preferable, to a non-dominated one in which the goal points of some objectives are not met (Fonseca & Fleming, 1995). All the preferred individuals thus achieve the same fitness, however the number of actual offspring may differ due to the stochastic nature of the selection mechanism. Thus an accumulation of the imbalances in reproduction can cluster the search into an arbitrary area of the trade-off surface. This phenomenon is known as genetic drift and can drastically reduce the quality and efficiency of the search. Proposed as a solution to genetic drift, fitness sharing penalizes the fitness of individuals in popular neighbourhoods in favour of more remote individuals of similar fitness.

Recombining arbitrary pairs of non-dominated individuals can result in the production of an unacceptably high number of unfit offspring, or lethals. A further refinement to the MOGA is therefore to bias the manner in which individuals are paired for recombination, often termed mating restriction. This restricts reproductions to individuals that are within a given distance of each other. Population diversity is maintained by adding random genetic information at each generation as well as mutating existing individuals. (see 'Add Random Immigrants' in Fig. 4 above)

The use of MOGA in tuning weighting functions for $H_\infty$-based controllers has proved successful when applied to a number of previous problems (Dakev et al 1997), (Griffin et al 1998), (Griffin et al 2001). This paper describes a preliminary investigation into extending this approach to using MOGA to tune the uncertainty and performance weighting functions during DK-iteration. In Fig. 5, a flowchart highlighting the fundamental steps involved in the evolutionary $\mu$-synthesis procedure is shown.

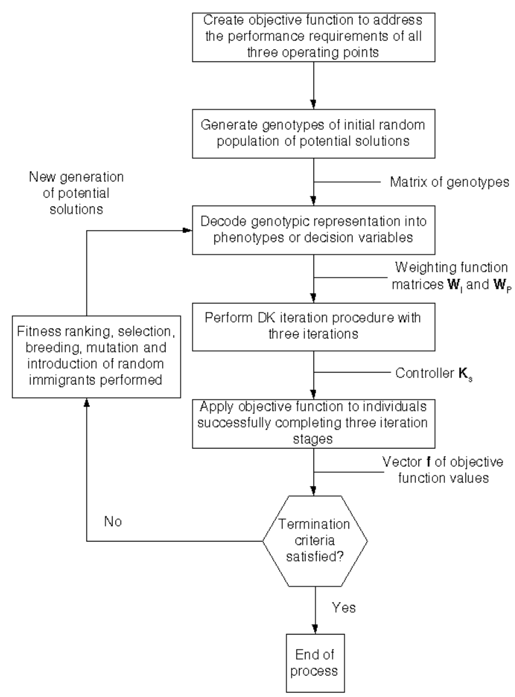


Fig. 5. Flow chart of the MOGA/$\mu$-synthesis controller design process.

## 5. GAS TURBINE ENGINE

This section describes the application of the MOGA/$\mu$-synthesis approach to the design of a controller for an aero gas turbine. A multiple model representation of the engine is used, with linear, time invariant models representing the engine at 100%, 95% and 90% of high pressure spool speed. Gas turbine engines traditionally use a loop selection strategy depending upon their operating condition (Astrom & Hagglund, 1995). Steady-state control is administered by different control loops to that used for transient control. Here, a control design is considered for a steady-state condition. The controller is a 2x2 multivariable controller using fuel flow and compressor variable guide vanes as inputs and thrust, P50, and intermediate pressure compressor speed, NI, as outputs. Due to limitations in the available model, the handling bleeds were designated as disturbance inputs via which disturbance events could be introduced into the system. The controller synthesis procedure was performed at the 100% high pressure spool speed operating point and the controller tested for robustness by assessing its performance at the other two operating points.

The optimization objectives chosen for this exercise can be seen in Table 1. The objective function values were produced in simulation using step and sine wave signals applied to the handling bleed inputs of the engine model. Table 1 lists the objectives used.

The weighting functions used to represent the plant uncertainty and performance requirements were diagonal matrices of first order lags of the structure a(bs + 1)/(cs + 1). The same parameters were used for both channels of the system for both the uncertainty and the performance. This was done in order to number of decision variables to a minimum for this initial investigation. The design procedure was a two-step process. Firstly, the MOGA was required to tune six decision variables, taking account of both the uncertainty and performance weighting functions. Once a robustly stable solution was available, this first MOGA was terminated. The parameters for the uncertainty weighing function were then declared as constants using the values from the chosen individual from the first MOGA. The second MOGA run was performed using only three decision variables for the performance weighting function, in an effort to optimise robust performance. The upper and lower bounds for the six decision variables were set as 0-100 for the gain, 0-7 for the lead time constant and 0-2 for the lag time constant.

## 6. GTE RESULTS

The performance of each candidate solution that is generated and assessed by the MOGA as displayed on a parrallel coordinates graph. The graph resulting from this design procedure is shown in Figure 6

| Obj. No. | Objective Description |
|---|---|
| 1 | Peak Fluctuation of P50 from 100% load O.P. |
| 2 | Peak Fluctuation of N2 from 100% load O.P. |
| 3 | Peak Fluctuation of P50 from 95% load O.P. |
| 4 | Peak Fluctuation of N2 from 95% load O.P. |
| 5 | Peak Fluctuation of P50 from 90% load O.P. |
| 6 | Peak Fluctuation of N2 from 90% load O.P. |
| 7 | Max. cont. eigenvalue of system |
| 8 | Mu robust performance measure, $\mu$ |

Table 1. GTE Controller Design Objectives

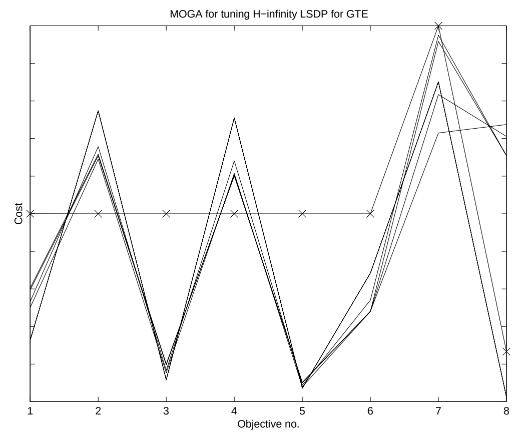


Fig. 6. Parallel co-ordinates graph for the GTE controller design procedure

The x-axis of the parrallel coordinates graph shows the objectives as described in Table 1. The y-axis shows the performance level for each objective, the scale being different for each. Each line represents the performance of a Pareto-optimal candidate solution with respect to the objectives shown along the x-axis. The crosses mark the performance goal for each objective. A line that achieves a value below the cross can be seen to have achieved the performance objective. Here, the performance objectives were maximum allowed fluctuations in P50 and NI for a bleed valve disturbance event. It can be seen that all lines in Figure 6 achived the P50 related targets with only small breaches of the NI related targets. The 8 objectives used in this problem were all equally weighted. A solution was selected from the graph and time plots were produced using the closed-loop representation in Simulink and those for the 100% and 90% operating points are shown in Figures 7, 8, 9, 10. Given that the controller design procedure was carried out at 100% and 90% is the furthest from that design point, these can be considered to be the nominal and worst-case responses of the closed-loop system. The closed-loop Simulink model is of the configuration shown in Figure 1.

The control performance for the GTE can be seen to be acceptable for the step and well as the sine wave disturbance events across the operating envelope being studied here. This is reflected by the

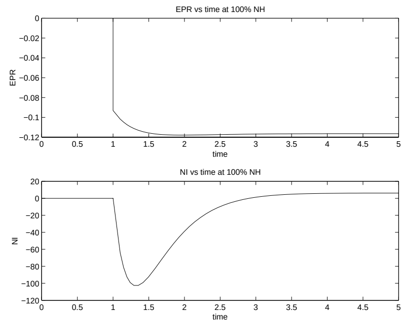


Fig. 7. Output responses to a step disturbance at 100% NH - $\mu$ controller

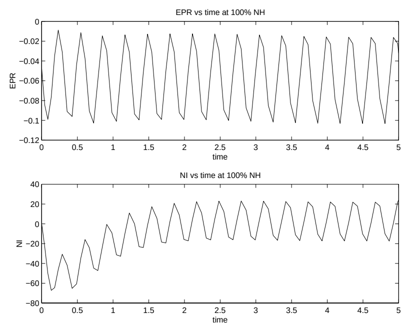


Fig. 8. Output responses to a sine wave disturbance at 100% NH - $\mu$ controller

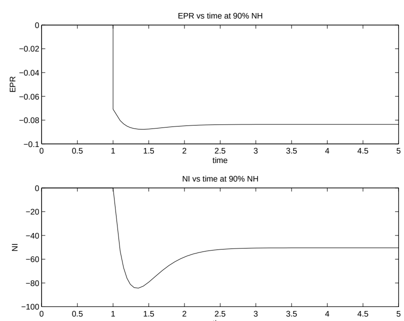


Fig. 9. Output responses to a step disturbance at 90% NH - $\mu$ controller

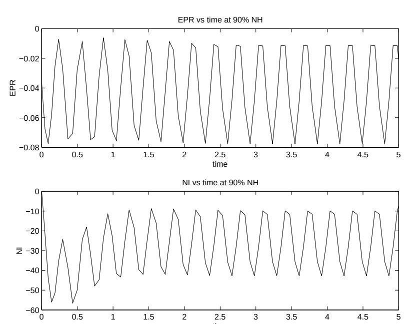


Fig. 10. Output responses to a sine wave disturbance at 90% NH - $\mu$ controller

$\mu$ value of the controller being $\mu = 0.99$ indicating an acceptable level of robust performance.

## 7. GASIFIER CONTROL REQUIREMENTS

Further to the study of the GTE, the use of multiobjective optimiser to tune the performance and uncertainty weighting functions during DK-iteration was investigated by designing a controller for a coal-burning gasification plant. The gasifier aims to burn coal in a clean, efficient manner to generate electricity. This problem was presented to British Universities as a Benchmark Challenge by a leading British energy producer (Griffin et al 1998).

A mixture of ten parts coal to one part limestone is pulverised and conveyed into the gasifier in a stream of air and steam. Once in the gasifier, the air and steam react with the carbon and other volatile elements in the coal. This reaction results in a low calorific value fuel gas and residual ash and limestone derivatives. This residue falls to the bottom of the gasifier and is removed at a controlled rate. The fuel gas escapes through an aperture at the top of the gasifier and is cleaned before being used to power a gas turbine.

The control design problem was to synthesise a controller at a single operating point that represented the highly non-linear gasifier at the 100% load case. Input and output constraints were specified in terms of actuator saturation and rate limits and maximum allowed deviation of controlled variables from the operating point. It was further specified that the controller developed should be tested at two other linear operating points. These represented the 50% and 0% load cases. This testing was to be performed off-line using the MATLAB/Simulink analysis and simulation package in order to assess robustness.

The gasifier was modelled as a 6-input, 4-output multivariable system. The inputs and outputs of the models are shown in Table 2 below.

| INPUT |
|---|
| 1 - WCHR - Char Extraction Flow (kg/s) |
| 2 - WAIR - Air Mass Flow (kg/s) |
| 3 - WCOL - Coal Flow (kg/s) |
| 4 - WSTM - Steam Mass Flow (kg/s) |
| 5 - WLS - Limestone Mass Flow (kg/s) |
| 6 - PSINK - Sink Pressure (N/m$^2$) |
| OUTPUT |
| 1 - CVGAS - Fuel Gas Calorific Value (J/kg) |
| 2 - MASS - Bed Mass (kg) |
| 3 - PGAS - Fuel Gas Pressure (N/m$^2$) |
| 4 - TGAS - Fuel Gas Temp. ($^o$K) |

Table 2. Table of Gasifier I/O

The state-space representations of the system are linear, continuous, time invariant models and have the inputs and outputs ordered as shown in Table 2. They represent the system in open-loop and are of 25th order.

The purpose of introducing limestone into the gasifier is to lower the level of harmful emissions. Limestone absorbs sulphur in the coal and therefore needs to be introduced at a rate proportional to that of the coal. It was specified that the limestone flow rate should be set to a constant ratio of 1:10, limestone to coal, making the limestone a dependent input. Given that PSINK is a disturbance input, this leaves four degrees of freedom for the controller design. The controller design can therefore be approached as a square, 4x4 problem.

The underlying objective of the controller design is to regulate the outputs during disturbance events using the controllable inputs. The outputs of the linear plant models are required to remain within a certain range of the operating point being assessed. These limits are expressed in units relative to the operating point and are therefore the same for all three operating points. They are as follows:

(1) The fuel gas calorific value (CVGAS) fluctuation should be minimized, but must always be less than +/-10KJ/kg.
(2) The bed mass (MASS) fluctuation should be minimized, but must always be less than 5% of the nominal for that operating point.
(3) The fuel gas pressure (PGAS) fluctuation should be minimized, but must always be less than +/-0.1bar.
(4) The fuel gas temperature (TGAS) fluctuation should be minimized, but must always be less than +/-1$^o$C.

The sink pressure (PSINK), represents the pressure upstream of the gas turbine which the gasifier is ultimately powering. Fluctuations in PSINK represent adjustments to the position of the gas turbine fuel value. It was specified that the value of PSINK should be adjusted in the following ways to generate disturbance events.

(1) Apply a step change to PSINK of -0.2 bar 30 seconds into the simulation. The simulation should be run for a total of 300 seconds.
(2) Apply a sine wave to PSINK of amplitude 0.2 bar and frequency 0.04Hz for the duration of the simulation. The simulation should be run for a total of 300 seconds.

### 7.1 *Evolutionary $\mu$-synthesis for the gasifier*

The design procedure for the gasification palnt was conducted as follows. Two disturbance conditions, a step of -0.2 bar and sine wave of amplitude 0.2 bar and frequency 0.04Hz, were applied to the closed-loop system at each operating condition using Simulink. Candidate solutions were generated by the MOGA in Matlab and these were passed to Simulink for the objective function values to be generated through simulation of the closed-loop system. A Simulink representation of the closed-loop system was used for each operating point and for each disturbance condition.

In order to apply the evolutionary $\mu$-synthesis approach to the gasifier, sixteen objectives were identified for the MOGA. A full listing of these objectives can be seen in Table 3. The principal objectives were those relating to the maximum fluctuation of each measured variable from the operating point. It has been found empirically, that framing the design criteria such that maximum fluctuations from the operating point are minimized, is most effective.

In addition to twelve primary objectives, four further objectives were identified as being desirable. The maximum continuous eigenvalue of the closed-loop system was minimised in order to maximise nominal stability. The $\mu$ value for robust performance was also optimised in an attempt to improve the characteristics of the resulting controller. It also became apparent during test runs of the optimisation that not all candidate solutions were suitable for the DK-iteration process when applied to the gasifier model. In order to address this problem, the optimiser attempted to maximise the number of iterations performed for each candidate solution up to a maximum of three. Any candidate solution that did not achieve three iterations was not assessed in terms of its control performance on the plant. The inclusion of this objective encouraged the population to evolve towards feasible areas of the solution space. Finally, the number of floating point operations performed by the machine when simulating the closed-loop system for each candidate solution is optimised. This objective was included in an attempt to avoid badly conditioned candidate solutions.

| Obj. No. | Objective Description |
|---|---|
| 1 | Peak fluctuation of CVGAS from 100% O.P. |
| 2 | Peak fluctuation of MASS from 100% O.P. |
| 3 | Peak fluctuation of PGAS from 100% O.P. |
| 4 | Peak fluctuation of TGAS from 100% O.P. |
| 5 | Peak fluctuation of CVGAS from 50% O.P. |
| 6 | Peak fluctuation of MASS from 50% O.P. |
| 7 | Peak fluctuation of PGAS from 50% O.P. |
| 8 | Peak fluctuation of TGAS from 50% O.P. |
| 9 | Peak fluctuation of CVGAS from 0% O.P. |
| 10 | Peak fluctuation of MASS from 0% O.P. |
| 11 | Peak fluctuation of PGAS from 0% O.P. |
| 12 | Peak fluctuation of TGAS from 0% O.P. |
| 13 | Max. cont. eigenvalue of system |
| 14 | Mu robust performance measure, $\mu$. |
| 15 | No. of successful DK-iterations |
| 16 | FLOPS (No. of floating point opertations) |

Table 3. Gasifier controller design objectives

The performance and uncertainty weighting functions were chosen to be diagonal matrices of first order transfer functions:- a(bs + 1)/(cs + 1).

This structure was chosen in order to minimise the complexity of the resulting $H_\infty$ controllers in the candidate solution set. A population size of 50 individuals was used and the maximum and minimum ranges for the parameters were chosen to be 0-100 for the gains, a, 0-7 for the lead time constants, b, and 0-2 for the lag time constants, c.

The 100% load linear model of the gasifier was used for the $H_\infty$ controller synthesis exercise. In order to run the DK-iteration process successfully, the order of the 100% gasifier model was reduced. Firstly, a minimal realisation was found, eliminating any uncontrollable or unobservable modes. This reduced the model from 25th order to 17th order. The model order was reduced still further using the Matlab 'modred' command to 4th order.

In order to produce the results for the gasifier, the MOGA was run in two stages. Firstly, the MOGA was configured in order to optimize the parameters for both the performance and uncertainty weighting matrices simultaneously. This meant that 24 parameters were optimized. Once a solution had been produced that exhibited suitable stability characteristics across the operating envelope of the gasifier, the first stage was terminated. The uncertainty weighting function parameters from this solution were then assumed to be a suitable representation of the variations in dynamics across the operating envelope. The MOGA was then re-run holding the uncertainty weighting matrix elements constant at these values and optimizing only the twelve parameters used for the performance weighting function matrix. This two-step approach was found to be the most effective way of producing a solution in a reasonable time frame.

### 7.2 *Gasifier Results*

The performance of each candidate solution that is generated and assessed by the MOGA as displayed on a parrallel coordinates graph. The graph resulting from this design procedure is shown in Figure **??**

The x-axis of the parrallel coordinates graph shows the objectives as described in Table 3. The y-axis shows the performance level for each objective, the scale being different for each. Each line represents the performance of a Pareto-optimal candidate solution with respect to the objectives shown along the x-axis. A solution was selected from the graph and time plots were produced using the closed-loop representation in Simulink and those for the 100% and 0% operating points are shown in Figures 12, 13, 14, 15

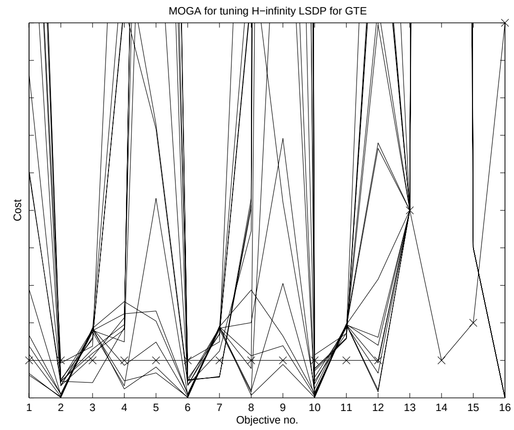


Fig. 11. Parallel co-ordinates graph for the gasifier controller design procedure

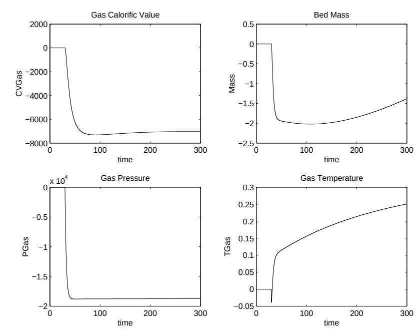


Fig. 12. Output responses to a step disturbance at 100% load - $\mu$ controller

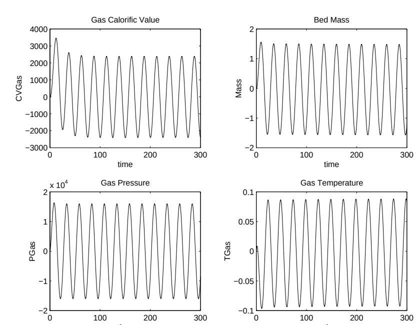


Fig. 13. Output responses to a sine wave disturbance at 100% load - $\mu$ controller

These results show that a controller has been produced that is stable across the operating range of the plant. This is confirmed by analysing the closed-loop eigenvalues. Performance is, however, poor for step responses particularly at the 0% load operating point. The design procedure has also resulted in a $\mu$ value of $\mu$=135.2. This confirms that the level of robust performance provided by the controller is not satisfactory in this case. This is reflected by the poor performance in response to a step in the disturbance signal.

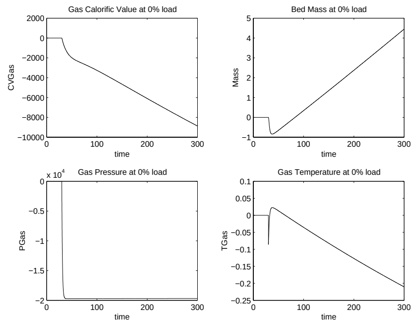


Fig. 14. Output responses to a step disturbance at 0% load - $\mu$ controller

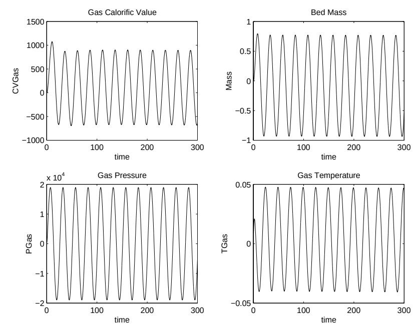


Fig. 15. Output responses to a sine wave disturbance at 0% load - $\mu$ controller

## 8. CONCLUSION

A preliminary investigation into the use of a multiobjective genetic algorithm for the tuning of uncertainty and performance weighting functions has been presented and applied to two case studies. The technique was further applied to the design of a controller for a gas turbine engine. Again, a multiple model representation was used with controller synthesis being performed at one operating point and robustness being assessed by applying the resulting controller to other operating points. The set of linear models for the GTE did not present the same scaling difficulties during the DK-iteration process as those for the gasifier, allowing a slight simplification of the design procedure in terms of the number of objectives used in the optimization. This resulted in an acceptable controller as shown by the attainment of a value of $\mu = 0.99$. Results for the coal-burning gasifier showed that this technique was capable of producing a stable, linear controller across a highly non-linear operating envelope. Performance levels were, however, not adequate at the operating point furthest from that at which the controller synthesis had been performed. This was reflected in an unacceptable value of $\mu = 135.2$.

It has been shown that this approach is capable of producing stable, robust linear controllers that can be applied to a non-linear operating envelope. Despite the unacceptable value of $\mu$ attained for the gasifier, the GTE case study demonstrates the ability of the approach to produce controller with a $\mu$ value less than 1, indicating acceptable levels of robust performance. It is therefore considered that this approach is worthy of further investigation. Further work will draw comparisons between the wholly MOGA-based approach and an approach where uncertailty weights are analytically produced.

## REFERENCES


K. J. Astrom, T. Hagglund, PID Controllers 2nd ed. Research Triangle Park, N.C. : International Society for Measurement and Control, 1995.

N. V. Dakev, J. F. Whidborne, A. J. Chipperfield , P. J. Fleming. Evolutionary $H_\infty$ design of an electromagnetic suspension control system for a maglev vehicle. *Proceedings of the Institute of Mechanical Engineers*, 1997, Volume 211, pp 345-55

J. C. Doyle, Analysis of Feedback Systems with Structured Uncertainties, *IEE Proceedings Part D*, 1982, Volume 129, Number 6, pp. 242-250

C. M. Fonseca, P. J. Fleming (1995). Multiobjective Genetic Algorithms made easy: Selection, sharing and mating restriction. *Evolutionary Computation. Proc 1st IEE/IEEE International Conference on Genetic Algorithms in Engineering Systems Innovations and Applications (GALESIA)pp 25-49.* Sheffield, U.K., pp 45-52.

I. A Griffin, P. Schroder, A. J. Chipperfield, P. J. Fleming (1998). Multiobjective Optimisation Approach to Gasifier Control, *MEC Benchmark Challenge on Gasifier Control: A One Day Seminar* Coventry, U.K., pp 200-207.

I. A Griffin, P. Schroder, A. J. Chipperfield, P. J. Fleming, (2001). Multiobjective Optimization approach to the ALSTOM gasifier problem. *Special Issue on the IMECHE Proceedings Part - I, Journal of Systems and Control Engineering ALSTOM Gasifier Control Engineering, Benchmark Challenge, Volume I,*

P. Schroder, B. Green, N. Grum, P. J. Fleming (1998). On-line genetic auto-tuning of PID controllers for an active magnetic bearing application. *5th IFAC workshop on Algorithms and Architectures for Real-Time Control*, Cancun, Mexico.

P. Schroder, A. J. Chipperfield, P. J. Fleming, N. Grum Robust Multivariable Control of Active Magnetic Bearings *Proc. European Control Conference Mechanical Engineers*, 1997, pp 1

S. Skogestad, I. Postlethwaite (1996). Multivariable Feedback Control: Analysis & Design John Wiley & Sons, Chichester, England